Chapter 2

EXPERIMENTAL AND THEORETICAL METHODS

In this chapter, the details of experimental methods and theoretical models used for understanding the phase stability of the chosen alloy systems are explained briefly. The equipment used in the synthesis and characterization of the prepared samples are discussed. Four HEAs are chosen in the present context. One quinary system from the most studied 3-d transition elements is chosen as CrFeCoNiCu HEA. The second alloy is a combination of lightweight components, i.e., MgAlMnFeCu HEA. The third and fourth alloys are refractory high entropy alloys as TiVZrMoW and TiVYZrHf HEAs. The first two alloys are synthesized by MA, while the high-temperature refractory alloys are synthesized by Vacuum arc melting. Phase evolution of all the alloys is studied using X-Ray diffraction (XRD), and Transmission electron microscope (TEM). The morphology, microstructural and elemental composition of as-milled and as-cast sample are studied using scanning electron microscopy (SEM) equipped with X-ray energy dispersive spectroscopy (EDS) and TEM-EDS techniques. The phase evolution of the synthesized alloys during time-temperature domain are investigated through in-situ high temperature XRD and differential scanning calorimetry (DSC).

2.1. Materials selection

The elemental powders of Mg, Al, Cr, Mn, Fe, Co, Ni, Cu, Ti, V, Y, Zr, Mo, Hf and W (purity $\geq$ 99.9 %) were used for the synthesis of four high entropy alloys. The physical properties of the elements are displayed in Table 2.1. The chosen elements belong to 3d-transition elements, non-transition elements (Mg and Al) and refractory transition elements.

Table 2.1: Physical properties of metals used for the synthesis of alloys.

Elements	Crystal Structure	Atomic Radius (Å)	Lattice Parameter (a,c) (Å)	Melting point (°C)	Electro-negativity	Density (g/cm^3)
Mg	HCP	1.73	3.21, 5.21	650	1.31	1.74
Al	FCC	1.43	4.05	660	1.61	2.7
Cr	BCC	1.28	2.88	1907	1.66	7.19
Mn	Cubic	1.61	8.89	1246	1.55	7.47
Fe	BCC	1.26	2.87	1538	1.83	7.87
Co	HCP	2.00	2.51, 4.07	1495	1.88	8.91
Ni	FCC	1.63	3.52	1455	1.91	8.90
Cu	FCC	1.40	3.61	1084	1.9	8.96
Ti	HCP	2.15	2.95, 4.68	1668	1.54	4.50
V	BCC	2.05	3.02	1910	1.63	6.11
Y	HCP	1.80	3.65, 5.73	1526	1.22	4.47
Zr	HCP	1.60	3.23, 5.14	1855	1.33	6.51
Mo	BCC	1.90	3.15	2623	2.16	10.28
Hf	HCP	2.25	3.20, 5.06	2233	1.3	13.31
W	BCC	2.10	3.16	3422	2.36	19.25

2.2 Synthesis routes

Two types of synthesis routes were adopted in the present investigation. The solid mixing route (Mechanical milling) and liquid mixing route (Vacuum arc melting). The first two HEAs (CrFeCoNiCu and MgAl MnFeCu) were synthesized by mechanical milling (MM) route, while the refractory high entropy alloys (TiVZrMoW and TiV YZrHf) were synthesized by vacuum arc melting.

Table 2.2: Milling parameters used for the synthesis of HEA powders.

Type of mills	High energy planetary ball mill (Retch PM 400 & 400/2)
Vials and Balls	Tungsten carbide (WC)
Ball diameter	10 mm
Ball to powder ratio (BPR)	10:1
Rotational speed	200 rpm
Process control agent (PCA)	Toulene
Milling medium	Wet
Running protocol	30 min stop after 1 h milling

2.2.1 Mechanical alloying

The powder particles of Cr, Fe, Co, Ni and Cu, and Mg, Al, Mn, Fe and Cu were taken in equiatomic proportion to synthesize the CrFeCoNiCu and MgAlMnFeCu high entropy alloys. The mechanical alloying was carried out in a high energy planetary ball mill (PM 400 & PM 400/2; Make: Retch, Germany) at 200 rpm with the ball to powder ratio (BPR) of 10:1. The elemental powders were milled in 250 ml tungsten carbide (WC) vials with WC balls of 10 mm diameter. In the present investigations, toluene was used as a process control reagent to avoid oxidation of powder particles during milling. The milling parameters are mentioned in **Table 2.2**. During the mechanical alloying, samples were withdrawn from the vials every 10 h to understand the phase evolution sequence due to structural transformation. Intermittently the high-energy planetary ball mill was stopped for 30 mins after every one h milling to avoid overheating during milling.

2.2.2 Vacuum arc melting

We have taken elemental powders of Ti, V, Mo, Zr, W, having purity above 99.9. The hydraulic press compresses the mechanical mixture of the elemental powders under a 2-tonne load to obtain a compressed pellet, which was then melted in a vacuum arc

furnace under an argon atmosphere. Before melting the actual compacted powder, the arc was struck onto a small Ti piece to ensure the absorption of any oxygen present in the chamber. The prepared alloy button was re-melted for five times, flipping the button each time to ensure proper homogeneity of the composition. The molten alloy is cooled using a water-cooled Cu crucible. Thus the cooling rate of the molten sample is fast, and there is a probability of finding high-temperature phases in the as-cast samples.

2.3 Structural characterization

In order to investigate the phase evolution process during mechanical milling, x-ray diffraction (XRD) was used, while transmission electron microscopy (TEM) is used to confirm the crystal structure of the final as-milled and as-cast samples. The microstructures of these alloys were examined through scanning electron microscopy and TEM. For the compositional analysis of the prepared alloys, techniques like SEM-EDS (x-ray energy dispersive spectroscopy) and TEM-EDS were used.

2.3.1 X-ray diffraction

The phase evolution of the CrFeCoNiCu HEA during milling of the powders was investigated through XRD (Rigaku, 40kV, 15mA) having Cu-K_α radiation (λ=0.154 nm) radiation. TiVZrMoW and TiVYZrHf HEAs were also scanned through the same instrument. The samples were examined in a 2θ range of $20°$ to $100°$ (for most samples) using a step size of $0.02°$ with a scan rate of $10°$ min^{-1}. The phase transformation in CrFeCoNiCu HEA as a function of temperature was investigated through in-situ XRD (Rigaku Smart Lab, 45 kV, 200 mA) having Cu-K_α radiation. The samples were scanned using a step size of $0.02°$ with a scan rate of $5°$ min^{-1}. The XRD instrument (EMPYREAN, PANalytical) was used for investigating the phases evolved during milling and spark plasma sintered compact of the milled powder.

2.3.2 Transmission electron microscopy

A transmission electron microscope (TEM) was used to investigate the crystal structures and fine microstructural features present in the alloy. TEM studies were performed by FEI Tecnai G2 T20, operated at 200 kV. This instrument is equipped with a high angle annular dark-field (HAADF) and EDS detector.

The powder samples of CrFeCoNiCu and MgAlMnFeCu were dispersed in ethanol. The ethanol and powder solution was ultra-sonicated for 20 minutes to avoid any accumulation of powder particles. This ethanol and powder suspension is drop cast on 3 mm copper grid (200 mesh size) and died with the help of an infrared lamp for 30 minutes. The as-cast sample of TiVZrMoW was brittle, handling thin foil become difficult. Thus the as-cast sample was crushed and milled for 15 min to get powder of the sample. Then this powdered sample was handled as described above for milled samples.

2.3.3 Scanning electron microscopy

The scanning electron microscope (SEM) is used for the characterization of microstructure at the nanometer range. The SEM instrument operates under two modes i.e., secondary electron (SE) mode and backscattered (BSE) mode. The SE mode is used for understanding the morphology of the grains within samples; on the other hand, chemical analysis is done using BSE mode.

The scanning electron microscope (FEI Quanta 200F, 20 kV) is used for the microstructural and compositional analysis of the as-milled CrFeCoNiCu and as-cast TiVZrMoW sample. The MgAlMnFeCu as-milled and sintered samples were investigated using NOVA NanoSEM 450, FEI operated at 30 kV. The powdered samples were sprinkled on the carbon tape attached to the SEM stub. The as-cast samples were first flattened by mechanical grinding of one of the surfaces using silicon carbide paper (60 μm grit size). After flattening the surface, samples were polished on emery paper (400 μm

to 2500 μm grit size). The samples' final polishing was done on ChemoMet cloth (trademark of Buehler) with colloidal alumina. Then the samples were etched with HF for revealing the grain boundaries.

2.4 Thermal stability

The alloys' thermal stability was investigated by differential scanning calorimetry (DSC) and annealing the samples at various temperatures. In CrFeCoNiCu alloy, the thermal stability was understood by in-situ XRD of the as-milled powder sample.

2.4.1 Differential scanning calorimetry

The thermal analysis of the mechanically alloyed MgAlMnFeCu alloy and as-cast TiVZrMoW alloy were done using a differential scanning calorimeter (DSC 404 F3 Pegasus, NETZSCH, Germany) under an inert atmosphere. This technique is used to determine the thermal changes in a material accompanied by an exchange of heat. Hence it helps in finding the transformation temperatures of the material. Alumina crucible was used as reference and sample holder. The sample holder was charged with ~20 mg of mechanically milled powder and an as-cast sample.

2.4.2 Annealing treatment

The heat treatments of the milled powder and as-cast alloy were carried out in the muffle furnace. The alloy samples were encapsulated in a quartz tube that is backfilled with argon. The vacuum arc melted samples (button) were cut into half for heat-treatments. These samples were kept in the furnace at different temperatures with a heating rate of $5°$ min^{-1}, followed by a definite holding time and furnace cooling.

2.5 Physical and mechanical behaviour

2.5.1 Hardness measurements

The bulk hardness of the SPSed samples of AlCuFeMnMg HEA was measured using a Vickers hardness tester (LECO LV700AT) at the load of 98 N with a dwell time

of 10 s. Five to ten readings were taken corresponding to each measurement, in order to compute the standard deviation. A microhardness tester (LM-248AT; LECO) was used to determine microhardness of the SPSed sample at an applied load of 430 mN with a dwell time of 5 s.

2.5.2 Compression testing

The compressive strength of MgAlMnFeCu HEA after SPS was determined using a 100 kN Universal Testing Machine (Model 4206, Instron). The compressive testing was performed at room temperature on cylindrical specimens prepared as per the ASTM E9-89a specification at a strain rate of 1.8×10^{-3} s^{-1}.

2.5.3 Density measurement

The density of spark plasma sintered MgAlMnFeCu HEA was measured by using Archimedes principle. The electronic weighing balance (Model No- CAH-503, CONTECH Instrument Ltd., Mumbai- INDIA) equipped with a density measurement kit was used for this purpose. The theoretical density of alloys was estimated by using the following relation-

$$\rho_t = x_1\rho_1 + x_2\rho_2 + x_3\rho_3 + \ldots\ldots + x_i\rho_i \qquad (2.4)$$

where x_i is the atomic concentration of ith element and ρ_i is the density of ith element.

2.6 Density functional theory

The density functional theory (DFT) is a part of the computational quantum mechanics and is also called *ab-initio* method [55]. This is used for finding the ground state of a collection of atoms by solving the many-body Schrodinger equation. The ground state of the group of atoms is used to predict the structural, vibrational, magnetic and electronic properties of materials. The Schrodinger equation is as given below:

$$\hat{H}\Psi(\{r_i\},\{R_I\}) = E\Psi(\{r_i\},\{R_I\}) \tag{2.5}$$

In this equation, $\hat{H} = \hat{T} + \hat{V}$ where $\hat{T}$ is the kinetic energy operator and $\hat{V}$ is potential energy due to Coulomb interaction between the pair of charged particles. r_i and R_I represent positions of electron and nuclei, respectively. To make this equation simple, the Born-Oppenheimer approximation is used [92]. According to this approximation, heavy nuclei move very slowly than fast-moving electrons, i.e., time taken by electrons to find ground state is much faster than the nucleus. Thus all the nuclei's are considered static, while electron interacts with the potential of static nuclei. Hence one wave function is decoupled into two wave functions ($\Psi(\{r_i\},\{R_I\}) \rightarrow \Psi_N(\{R_I\}) * \Psi_e(\{r_i\})$). Now we have to find the ground state energy of electrons only. So the Schrodinger equation [93] for electrons can be represented as

$$\hat{H} = -\frac{h^2}{2m_e}\sum_i^{N_e}\nabla_i^2 + \sum_i^{N_e}V_{ext}(r_i) + \sum_{i=1}^{N_e}\sum_{j>1}U(r_i,r_j) \tag{2.6}$$

In the above equation, the first part represents the kinetic energy of the electrons. The second and third parts describe the interaction between nucleus-electron and electron-electron, respectively. Now we have three spatial dimensions per electron position. Thus solving equations for a system with 20 electrons will become a 60-dimensional problem. The problem of dimensionality is simplified by defining an electron density function represented by n(r) [$n(r) = \Psi^*(r_1,r_2,r_3,........r_N) * \Psi(r_1,r_2,r_3........r_N)$]. Considering this reduces the 3N dimensional problem to only 3 spatial dimensions. Thus, the many-electron problem is reduced to many one-electron problems, i.e., any jth electron is treated as a point charge in the field of all other electrons [$\Psi(r_1,r_2,r_3,........r_N) = \Psi(r_1) * \Psi(r_2) * \Psi(r_3) * ....\Psi(r_N)$]. This product is also known as Hartree product [94].

2.6.1 DFT: From wave functions to electron density

The first principles calculation, if done using electron density, is known as DFT. This calculation is based on the two basic theorems given by Hohenberg and Kohn. The theorems state as

Theorem 1: The ground state energy E is a unique functional of electron density $E = E[n(r)]$ [56].

Theorem 2: The electron energy that minimizes the energy of the overall functional is the true electron density corresponding to the full solution of the Schrodinger equation [56]. The energy functional term in the Schrodinger equation can be expanded as

$$E[\{\Psi\}] = E_{known}[\{\Psi_i\}] + E_{XC}[\{\Psi_i\}] \tag{2.7}$$

$E_{known}[\{\Psi_i\}] =$ K.E. of electrons + P.E. between electron and nucleus + electron-electron repulsion + nucleus-nucleus repulsion.

$E_{XC}[\{\Psi_i\}] =$ exchange correlation functional. This exchange correlation functional includes all quantum mechanical terms, which needs to be approximated for the solution. Two most commonly used exchange correlation functionals are local density approximation (LDA) and generalized gradient approximation (GGA).

2.6.2 Kohn-Sham scheme

Solve the Kohn-Sham equation for each electron having three spatial variables $\Psi_i(r)$, namely,

$$\left[-\frac{h}{2m}\nabla^2 + V(r) + V_H(r) + V_{XC}(r) \right]\Psi_i(r) = \varepsilon_i(r) \tag{2.8}$$

where the first three terms in the brackets represent kinetic energy of electron, interaction between electron and nucleus and Hartree product respectively [95]. Here, $V_{XC}(r)$

represents exchange correlation potential. An iterative scheme is used to solve Schrodinger equation in a self-consistent manner as given below:

1. An arbitrary electron density n(r) is initially chosen for the selected system. This electron density is usually chosen by software such as VASP or Quantum ESPRESSO.

2. The Kohn-Sham equation is solved using the n(r) chosen in step 1. By solving this equation we obtain set of single electron wave functions $\Psi_i(r)$.

3. The new electron density n'(r) is calculated using new set of electron wave functions

$$n'(r) = 2\sum_i \Psi_i^*(r)\Psi_i(r) \tag{2.9}$$

4. If new $n'(r)$ is significantly different from the starting n(r) then steps 2 and 3 are carried out using new $n'(r)$. If new $n'(r)$ and starting n(r) are same within some tolerance limits, then the true ground state density is obtained.

2.7 Special quasirandom structure (SQS)

The *ab-initio* method based on the Kohn-Sham theorem of DFT is a powerful tool for predicting the formation of phases and their stability under different conditions. The only input needed for the calculation is the crystal geometry of the phases. In case of multicomponent systems, like in HEAs, the design and analysis of a disordered multicomponent solid solution are challenging. If the number of atoms in the chosen system increases, the computational time and cost also increases exponentially. The disordered solid solution cell can be designed mainly by Coherent Potential Approximation (CPA) [96], Special Quasirandom Structure (SQS) [97], and Cluster Expansion method [98]. SQS generates a supercell that closely relates to the correlation function of a completely disordered solid solution. As the computational cost increases

with the increase in the size of a supercell, a small SQS is preferred for computational efficiency [99]. However, in multicomponent systems (≥ 4), it becomes a challenging task to model small-sized SQS that mimics disordered solid solution.
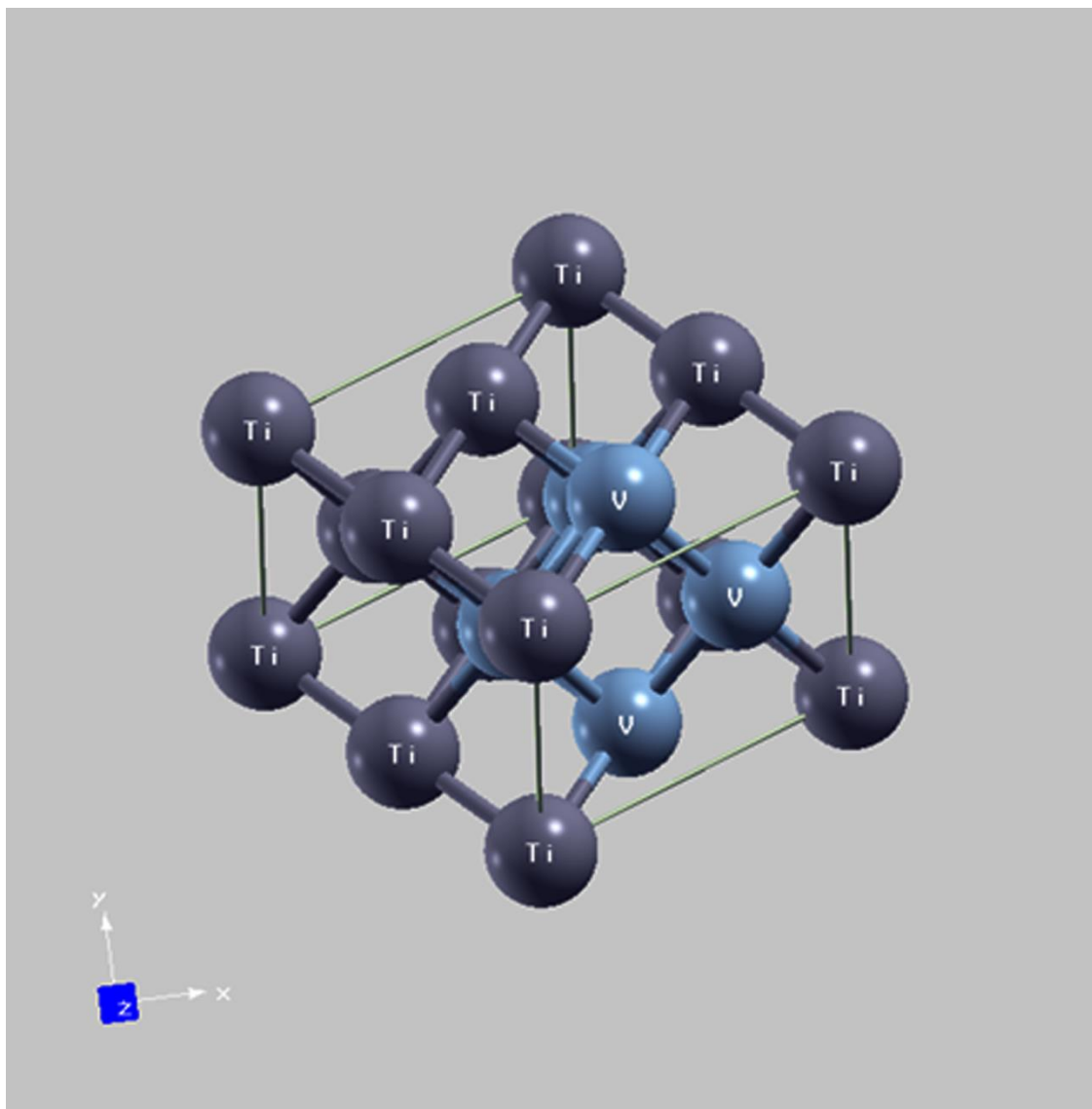

Figure 2.1: A representative picture of randomly distributed Ti and V atom over 8 atom cell (SQS-8) used in the calculation of formation energy for Ti-V binary systems.

We have attempted to calculate the enthalpy values of binary subsystems more accurately by using DFT. An eight atom SQS is generated using Alloy Theoretic Automated Toolkit (ATAT) [100] for all the binary subsystems, as shown in **Figure 2.1**.

The enthalpies of mixing for BCC, FCC, and HCP crystal structures for all the binary subsystems are calculated using Quantum ESPRESSO (opEn-Source Package for Research in Electronic Structure, Simulation, and Optimization) code that works on DFT using the plane wave method. Generalized gradient approximation [101] is used under Perdew-Burke-Ernzerh (GGA-PBE) [102] to calculate exchange-correlation. More wave functions were allowed in the calculation by increasing the cut-off energy of binary systems by 25%. Monkhorst-pack scheme [103] is used for K-points sampling in the Brillouin zone of reciprocal space. All the SQSs are volume relaxed in the present work to find the lowest energy configuration. The BFGS quasi-newton algorithm does the relaxation of the supercell. Accuracy of the current calculations is verified by calculating the elements lattice parameters and comparing them with the experimental lattice parameters.

2.8 Cluster expansion (CE) method

In many materials, there are various phases defined by an underlying spatial lattice (e.g., BCC, FCC for many metal alloys). The stability of these various phases is determined by the relative energy of the specific arrangement of the individual atoms on a given lattice type and can change with concentration. In the cluster expansion method, because the underlying spatial lattice type remains largely constant around the original positions of the nuclear coordinates (R_1……R_m), we can focus on what happens to the total energy (or relative energy) if we replace some atoms of a given species with another atom species for the set of known atomic positions in the crystal. In this case, the energy (E) becomes a simple function of the occupation of these sites by the different chemical species (Z):

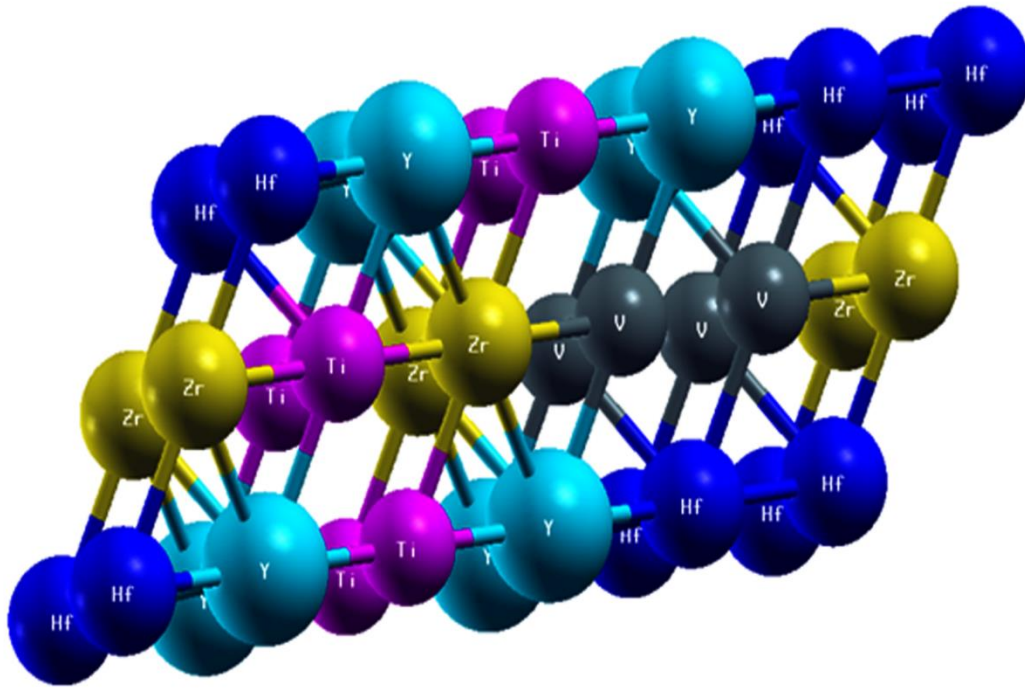$$E(R_1,..........,R_m) = E_{conf}(Z_1,........,Z_m)$$ (2.10)

Figure 2.2: A representative structure of 10 atom primitive BCC cell over which 5 elements are distributed.
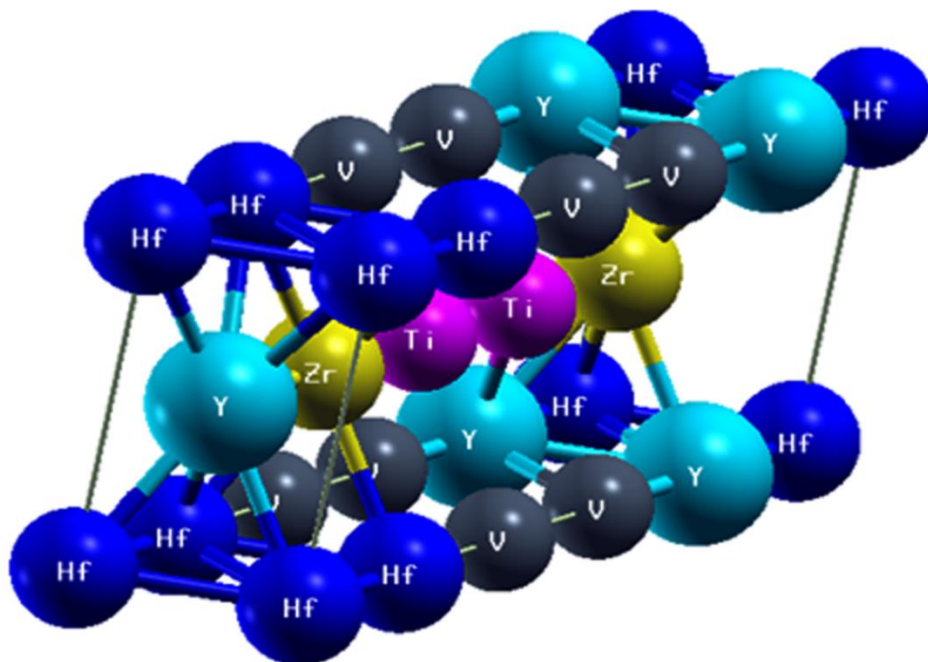

Figure 2.3: A representative structure of 10 atom primitive HCP cell over which 5 elements are distributed.

We have attempted to modify the cluster expansion method by choosing a cell with fixed composition and lattice sites. A 10 atom primitive cell of BCC and HCP was chosen and 5 elements were distributed over 10 sites. The total number of ways to arrange 5 elements over 10 atom sites is 1,13,400. A total of 22,680 structures were obtained by removing the equivalent structures from the list. In a 10 atom BCC primitive cell we have considered pairs (up to 3rd neighbours) and triangle interactions to obtain distinct structures. Thus, the number of distinct working configurations reduced to 5925. For HCP 10 atom cell, we have only considered pair interactions up to 3rd neighbour pair resulting in 11,040 distinct structures. Representative cells in BCC and HCP structures are shown in **Figure 2.2** and **2.3** respectively.

Before starting the calculations for the alloy systems, we have optimized the values of energy cut-off (E_{cut}), k-points and the lattice parameters of the individual elements. The energy cut-off of the calculations is fixed by converging the total energy of the elements with respect to increasing E_{cut} value. Similarly the k-points samplings must be tested with respect to energy convergence. The optimization of the energy cut-off and k-points are needed because with increasing values of these parameters accuracy improves but at the cost of more computational time (calculation time increases exponentially). The optimized values of E_{cut} and k-points used in the calculations of the energies of TiVZrYHf are 45 Ry and 10x10x10 (in x, y, and z directions), respectively.

2.9 CALPHAD approach

Many CALPHAD databases have been developed based on single principal element which can assess the Gibbs energies of the systems. A careful thermodynamic assessment of binary and ternary subsytems are sufficient to describe the thermodynamic properties of quaternary and higher order systems. This is because the probability of the

occurrence of quaternary and higher order intermetallic phases is minimal [104]. Thus, thermodynamic assessment of binary and ternary subsystems is sufficient for the prediction of thermodynamic properties of quaternary and higher systems by extrapolation from the binary and ternary subsystems. As most of the databases do not have complete thermodynamic assessment of all binary and ternary assessments, a complete thermodynamic description is currently unavailable for a huge number of quaternary (or higher order) alloy systems, which may have a potential practical interest.

We have used the solid solution database (SSOL-5) for the prediction of phases, volume fraction of phases and phase transformation temperatures of the chosen alloy. We have also calculated the binary phase diagrams of the binary subsystems, to investigate the high and low temperature phases present. We have checked the presence of those phases either by experimental methods or theoretical computations or by both.